Published in final edited form as:
Adv Healthc Mater. 2013 September ; 2(9): 1204–1208. doi:10.1002/adhm.201200381.

Triggered Drug Release from Superhydrophobic Meshes using High-Intensity Focused Ultrasound

Stefan T. Yohe,
Department of Biomedical Engineering and Chemistry, Boston University, Boston, MA 02215

Jonathan A. Kopechek,
Department of Biomedical Engineering and Mechanical Engineering, Boston University, Boston, MA 02215

Tyrone M. Porter,
Department of Biomedical Engineering and Mechanical Engineering, Boston University, Boston, MA 02215

Yolonda L. Colson, and
Division of Thoracic Surgery, Department of Surgery, Brigham and Women's Hospital, Boston, MA 02215

Mark W. Grinstaff
Department of Biomedical Engineering and Chemistry, Boston University, Boston, MA 02215

Mark W. Grinstaff: mgrin@bu.edu

Abstract

Application of high-intensity focused ultrasound to drug-loaded superhydrophobic meshes affords triggered drug release by displacing an entrapped air layer. The air layer within the superhydrophobic meshes is characterized using direct visualization and B-mode imaging. Drug-loaded superhydrophobic meshes are cytotoxic in an *in vitro* assay after ultrasound treatment.

Keywords

biomaterials; HIFU; superhydrophobic; triggered; ultrasound; drug delivery; electrospinning; meshes

The current standard of care for many ailments relies on a bolus of a pharmacologic agent which is delivered orally, intravenously, or via a local injection. These delivery options offer minimal control over how much drug arrives at a target site and over what time period, and instead, duration and dose is dictated by the intrinsic pharmacokinetic/pharmacodynamic profiles of these agents. For indications such as cancer, non-targeted, highly toxic chemotherapeutic drugs (e.g., irinotecan and paclitaxel) are traditionally used, and systemic morbidity resulting from toxicity to healthy tissue is a significant concern. Consequently, approaches to target drug delivery to a specific site are highly sought-after.[1–8] These approaches generally fall into two categories: 1) particulate-based systems, with a bioactive agent loaded within nano- or micro- sized structures; and 2) localized drug depots implanted at the site of interest. Particles are frequently modified to possess ligands that bind an up-

Correspondence to: Mark W. Grinstaff, mgrin@bu.edu.

Supporting Information
Supporting Information is available from the Wiley Online Library or from the author.

regulated receptor present on a tumor,[9–13] or alternatively, are activated by a stimulus (electric field, enzymatic degradation, magnetic field, heat, ultrasound, oxidative stress, light)[14–21] to localize and/or trigger drug release at a specific location. Our interest is in triggered delivery via an external stimulus. Thermal-responsive doxorubicin-loaded liposomes represent an example of this approach which has successfully translated to clinical evaluation (ThermoDox, Phase III clinical trial) for the treatment of liver cancer.[22] After i.v. administration, radio frequency ablation of the tumor causes direct thermal damage while simultaneously activating liposomes to release their drug payload at the target site.

In contrast to particle-based strategies, localized drug depots[8, 23] traditionally do not use additional targeting/triggering methods as they are implanted locally at the site of disease to obviate this need. These devices, once implanted, offer limited control over release, predominantly relying on passive diffusion of a bioactive agent out of a polymer matrix over a defined period of time. However, there exists a strong clinical need for triggered drug delivery from implantable devices in applications such as locoregional treatment of cancer. For example, the ability to trigger release of a chemotherapeutic agent from a drug depot after surgical resection of a tumor, once wound healing has been confirmed or an infection treated, would be clinically advantageous.[24–26] We recently reported the use of 3D superhydrophobic meshes for drug delivery, where air is entrapped both at the material surface and within the 3D structure.[27] Changes in the stability of the superhydrophobic state result in differences in the rate of air displacement by water, which affords control over the rate of drug release. We hypothesized that release from superhydrophobic meshes could be triggered using ultrasound, where the pressure wavefront removes the air layer. Figure 1A illustrates this concept, where drug release is triggered by propagation of the sound waves through the medium to the mesh via ultrasound treatment. Herein, we describe fabrication of functional drug-loaded superhydrophobic 3D meshes, characterization of the robustness of the entrapped air layer with acoustic pressure delivered by high-intensity focused ultrasound (HIFU), evaluation of drug release with and without ultrasound treatment, and assessment of cytotoxicity before and after triggered drug elution.

Three-dimensional superhydrophobic meshes were fabricated by electrospinning poly(ε-caprolactone) (PCL) and poly(glycerol monostearate-co-caprolactone) (1:4) (PGC-C18) (Figure 1 B–C).[28–29] Electrospinning produces a high surface area material, and PGC-C18 doping decreases surface energy, both of which are requisite properties to achieve superhydrophobicity. Specifically, doping of PGC-C18 (30 wt%) led to high apparent contact angle (ACA) meshes (153°), both due to a decrease in surface energy and an increase in surface roughness (reduction in fiber size, fill fraction). This combination of surface chemistry and material roughness of PCL with 30% PGC-C18 supports a stable air layer (a stable Cassie-Baxter state) within the bulk material with the selected electrospinning conditions to yield a superhydrophobic 3D material.[27] Less PGC-C18 doping (<25 wt%) at the same electrospinning conditions resulted in meshes with a less stable air pocket.

Electrospun PCL (ACA = 121°), PCL with 10% PGC-C18 (ACA = 143°), and PCL with 30% PGC-C18 (ACA = 153°) were fabricated as representative 3D superhydrophobic meshes with entrapped air spanning the range from weakly metastable to stable when submerged in water. The removal of air from each of these meshes was studied using a three-prong approach after HIFU treatment: direct optical visualization, quantification of total wetted area, and B-mode imaging. Wetting of superhydrophobic PCL meshes was directly visualized as shown in Figure 2, where before treatment meshes were opaque with an entrapped air layer, and light is scattered/reflected. Meshes were bound to a plastic holder, submerged in water, and with application of a sufficient acoustic pressure using HIFU resulted in removal of the entrapped air. Water infiltration was visualized directly by removal of the air bubbles, as well as increased transparency at the site of treatment.

The video recordings taken during HIFU treatment were subsequently analyzed to determine the total wetted area of 3D superhydrophobic meshes. A reference frame of meshes before treatment was used for background subtraction, and the resultant change in image intensity after HIFU treatment was used to calculate the total wetted area. HIFU treatment was performed for 10 seconds in continuous wave (CW) mode or pulsed mode (center frequency of 1.1 MHz, pulse duration of 10 cycles, pulse repetition frequency of 50 Hz) on PCL, PCL with 10% PGC-C18, and PCL with 30% PGC-C18 meshes with peak rarefaction pressures (P_{pk}) ranging from 0.71 – 4.25 MPa. Undoped PCL meshes were easily wetted by HIFU in CW mode with P_{pk} of 1.06 MPa and higher, with a linear increase in the wetted area (Figure 3A). With application of 4.25 MPa of pressure, a maximum area of 11.6 mm^2 was wetted. Superhydrophobic meshes containing 10% or 30% PGC-C18 required a 3 to 4 fold increase in applied pressure to remove the entrapped air and induce wetting. With 10% PGC-C18 doping, the minimum applied P_{pk} required to achieve wetting was 3.54 MPa, with significant wetting observed at P_{pk} = 4.25 MPa (14.8 mm^2). With 30% PGC-C18 doping, only a modest amount of wetting was present at even the highest pressures used (1.17 mm^2 at 4.25 MPa). Significantly different results were obtained when using HIFU in pulsed mode. With the addition of any PGC-C18 to PCL meshes, no wetting was observed in pulsed mode (Figure 3B). PCL meshes, which did not contain PGC-C18, still wetted at all intensities, but show ≈10-fold less wetting compared to CW mode. The decrease in wetting with pulsed mode compared to CW mode suggests that removal of entrapped air is also a function of the total ultrasound exposure time. While the P_{pk} are the same for both treatments, the total time of ultrasound transmission was 22,000 times greater in CW mode than in pulsed mode.

It was also possible to detect removal of the air from the meshes due to HIFU treatment using B-mode imaging (VisualSonics, Inc, 55 MHz scanhead). Without wetting, images of submerged meshes had a bright interface, where the entrapped air highlighted the surface rather than the underlying porous 3D structure. However, the bulk mesh was easily visualized after removal of the entrapped air layer using HIFU, where the material appeared bright, as the electrospun fibers within the mesh created a large degree of scatter (Figure 4). The weakly metastable entrapped air in the PCL meshes was fully removed after HIFU exposure and the entire mesh was visualized. With 30% PGC-C18 addition to PCL, the majority of air was removed, but some air bubbles/pockets remained and prevented full transmission of ultrasound for visualization of the hydrophobic mesh. Because triggered drug release from the superhydrophobic meshes is based upon removal of the highly echogenic air within the mesh, it may be possible to detect the onset of triggered drug release with clinical B-mode ultrasound imaging (*i.e.* change in echogenicity of the mesh). This would be an advancement over current ultrasound-triggered drug release systems.[30–32]

Next, HIFU treatment was used as a trigger to initiate drug release from the superhydrophobic meshes. SN-38 (7-ethyl-10-hydroxycamptothecin) was selected as a model drug for use in these studies due to our previous experience working with camptothecins,[33–34] its potency in treating many cancer types,[35–36] the relative ease in detecting low quantities (<1 ng/mL), and it is the active metabolite of irinotecan. SN-38 (0.1 wt% and 1 wt%) was encapsulated into PCL with 30% PGC-C18 meshes, which have a stable air layer over several months (>10 weeks) when placed in an aqueous solution.[27] In the first study, less than 10% of SN-38 was released over 35 days without ultrasound treatment for meshes containing 0.1% or 1% SN-38 (Figure 5A), consistent with our earlier report. However, with the application of HIFU (P_{pk} = 4.25 MPa CW) at day 7, drug release was initiated as water infiltrated into the superhydrophobic meshes. More than 50% of total encapsulated SN-38 was released within 14 days after ultrasound treatment, followed by a slower, steady release of the remaining drug which concluded 28 days after treatment.

Similar drug release profiles were observed for both 0.1 % and 1% SN-38 concentrations. To further confirm that the displacement of air leads to subsequent drug release, an ethanol dip study was performed. Dipping in ethanol led to immediate removal of the air layer, as the surface tension of ethanol is significantly lower than water (22 vs. 72 mN/m). After a 5 second ethanol dip, meshes released SN-38 with an initial burst (>30% SN-38 in 2 days), with remaining drug released linearly over 4 weeks.

Next, the drug release study was repeated in the presence of serum, as proteins including albumin will likely modify the release properties.[37] Surfactants are well known to reduce the surface energy of a superhydrophobic surface through binding events of their hydrophobic domains, as well as reduction of the surface tension of water at the interface, both of which can lead to greater ease in removing entrapped air. A 10% serum supplementation was selected to allow comparison between the drug release and cell culture studies. When performing release in 10% serum, the air layer in meshes containing 30% PGC-C18 was no longer fully stable (Figure 5B), with prolonged linear release over 35 days. However, the entrapped air layer still slowed water penetration compared to the fully wetted ethanol case (40% vs. 58% released at 14 days). One strategy to mitigate release in the presence of biological surfactants is to use a layer-by-layer construct, where two non-drug loaded layers sandwich the drug containing layer and act as a superhydrophobic barrier to effectively prevent release. We fabricated a layer-by-layer construct with a 100 μm SN-38-loaded interior, sandwiched between two non-drug loaded 120 μm meshes. All of the layers were created from PCL with 30% PGC-C18. For the first 14 days, no drug release was observed for untreated meshes (0% SN-38 release/day), with minimal drug release after (13% at 35 days, or 0.6% SN-38 release/day post day 14) in the presence of serum. Following HIFU exposure at day 7, drug release was initiated (33% SN-38 in 5 days), with remaining drug released by 28 days (3% SN-38 release/day post HIFU treatment at day 7). Differences in SN-38 release rates from layered meshes before and after HIFU treatment were statistically significant using an analysis of covariance (ANCOVA) ($p=0.0012$).

Finally, we evaluated the layer-by-layer superhydrophobic meshes containing 1% of SN-38 in an *in vitro* cell assay using a human breast cancer cell line (MCF-7) in 10% serum-containing media. Cells incubated with SN-38-loaded meshes that did not receive an HIFU treatment, or empty non-drug loaded meshes, were viable for the entire 15 day study (Figure 6). Cells incubated with SN-38 loaded meshes prior to HIFU treatment were also fully viable, but demonstrated over 90% cytotoxicity immediately after HIFU treatment ($p<0.0001$). Meshes were not incubated with cells while receiving HIFU treatment to trigger drug release.

IFU is currently used clinically for the treatment of uterine fibroids[38], and is emerging as an attractive method for selective ablation of inoperable tumors with the ability to direct treatment with magnetic resonance imaging (MRI).[39–41] We have shown that superhydrophobic meshes have a stable air layer until destabilized with the use of HIFU, allowing localized triggered drug release. This is a significant distinguishing feature from other implantable drug depots where no or minimal control over release is afforded after implantation. Furthermore, the disruption of the air layer and associated triggered drug release can be monitored with clinical diagnostic ultrasound, which is a desirable feature for clinical utility. Triggered drug release from superhydrophobic meshes may be considered for concurrent use with tissue ablation in these mentioned indications, or instead in the treatment of separate pathologies such as recurrent cancer. The implantation of meshes during tumor resection would provide sufficient time for wound healing immediately following surgery with minimal drug release, with subsequent ultrasound triggering to initiate localized therapy to prevent recurrence. As we are at the initial stages of this research, a number of studies are planned to further evaluate these meshes with

identification of the advantages and limitations of these materials including drug release as a function of serum concentration, the effect of dissolved gases on drug release, and performance in an *in vivo* murine tumor model. In summary, the 3D superhydrophobic meshes discussed allow triggered removal of air on demand using ultrasound, which is interesting as a method for triggered drug delivery and broadly applicable to a variety of existing and emerging applications.

Supplementary Material

Refer to Web version on PubMed Central for supplementary material.

Acknowledgments

This work was supported in part by BU Training Grant in Pharmacology and Experimental Therapeutics, BU MSE Innovation Grant, BU Nanotheranostics ARCBWH, CIMIT, ARRC Ultrasound Micro-Imaging Core at BUSM, Boston University's Nanomedicine Program and Cross-Disciplinary Training in Nanotechnology for Cancer NIH R25 CA153955, and NIH R01CA149561. Supporting Information is available online from Wiley InterScience or from the author.

References

1. Davis ME, Chen Z, Shin DM. Nat. Rev. Drug Discov. 2008; 7:771. [PubMed: 18758474]
2. Malam Y, Loizidou M, Seifalian AM. Trends Pharmacol. Sci. 2009; 30:592. [PubMed: 19837467]
3. Petros RA, DeSimone JM. Nat. Rev. Drug Disco. 2010; 9:615.
4. Kim S, Kim J-H, Jeon O, Kwon IC, Park K. Eur. J. Pharm. Biopharm. 2009; 71:420. [PubMed: 18977434]
5. Brigger I, Dubernet C, Couvreur P. Adv. Drug Deliver. Rev. 2002; 54:631.
6. Lee CC, MacKay JA, Frechet JMJ, Szoka FC. Nature Biotechnol. 2005; 23:1517. [PubMed: 16333296]
7. Wolinsky JB, Grinstaff MW. Adv. Drug Deliver. Rev. 2008; 60:1037.
8. Wu P, Grainger DW. Biomaterials. 2006; 27:2450. [PubMed: 16337266]
9. Byrne JD, Betancourt T, Brannon-Peppas L. Adv. Drug Deliver. Rev. 2008; 60:1615.
10. Danhier F, Feron O, Préat V. J. Control. Release. 2010; 148:135. [PubMed: 20797419]
11. Gu FX, Karnik R, Wang AZ, Levy-Nissenbaum E, Hong S, Langer RS, Farokhzad OC. Nanotoday. 2007; 2:14.
12. Moghimi SM, Hunter AC, Murray JC. Pharmacol. Rev. 2001; 53:283. [PubMed: 11356986]
13. Rothenfluh DA, Hubbell JA. Integr. Biol. 2009; 1:446.
14. Sun C, Lee JSH, Zhang M. Adv. Drug Deliver. Rev. 2008; 60:1252.
15. Chilkoti A, Dreher MR, Meyer DE, Raucher D. Adv. Drug Deliv. Rev. 2002; 54:613. [PubMed: 12204595]
16. Ganta S, Devalapally H, Shahiwala A, Amiji M. J. Control. Release. 2008; 126:187. [PubMed: 18261822]
17. Pitt WG, Husseini GA, Staples BJ. Expert Opin. Drug Del. 2004; 1:37.
18. Qiu Y, Park K. Adv. Drug Deliv. Rev. 2001; 53:321. [PubMed: 11744175]
19. Shum P, Kim JM, Thompson DH. Adv. Drug Deliver. Rev. 2001; 53:273.
20. Mitragotri S. Nature Rev. Drug Discov. 2005; 4:255. [PubMed: 15738980]
21. Ferrara KW. Adv. Drug Deliver. Rev. 2008; 60:1097.
22. Landon CD, Park JY, Needham D, Dewhirst MW. Open Nanomed. J. 2011; 3:38. [PubMed: 23807899]
23. Wolinsky JB, Colson YL, Grinstaff MW. J. Control. Release. 2012; 159:14. [PubMed: 22154931]
24. Liu R, Wolinsky Jesse B, Catalano Paul J, Chirieac Lucian R, Wagner Andrew J, Grinstaff Mark W, Colson Yolonda L, Raut Chandrajit P. Ann. Surg. Oncol. 2012; 19:199. [PubMed: 21769471]

25. Wolinsky JB, Liu R, Walpole J, Chirieac LR, Colson YL, Grinstaff MW. J. Control. Release. 2010; 144:280. [PubMed: 20184934]
26. Liu R, Wolinsky JB, Walpole J, Southard E, Chirieac LR, Grinstaff MW, Colson YL. Ann. Surg. Oncol. 2010; 17:184.
27. Yohe ST, Colson YL, Grinstaff MW. J. Am. Chem. Soc. 2012; 134:2016. [PubMed: 22279966]
28. Wolinsky JB, Yohe ST, Colson YL, Grinstaff MW. Biomacromolecules. 2012; 13:406. [PubMed: 22242897]
29. Wolinsky JB, Ray WC III, Colson YL, Grinstaff MW. Macromolecules. 2007; 40:7065.
30. Kim HJ, Matsuda H, Zhou H, Honma I. Adv. Mater. 2006; 18:3083.
31. Kwok CS, Mourad PD, Crum LA, Ratner BD. J. Biomed. Mater.Res. 2001; 57:151. [PubMed: 11526905]
32. Norris P, Noble M, Francolini I, Vinogradov A, Stewart P, Ratner B, Costerton J, Stoodley P. Antimicrob. Agents Ch. 2005; 49:4272.
33. Wolinsky JB, Liu R, Walpole J, Colson YL, Grinstaff MW. J. Control. Release. 2010; 17:1203.
34. Morgan MT, Nakanishi Y, Kroll DJ, Griset AP, Carnahan MA, Wathier M, Oberlies NH, Manikumar G, Wani MC, Grinstaff MW. Cancer Res. 2006; 66:11913. [PubMed: 17178889]
35. Mathijssen RHJ, Van Alphen RJ, Verweij J, Loos WJ, Nooter K, Stoter G, Sparreboom A. Clin. Cancer Res. 2001; 7:2182. [PubMed: 11489791]
36. Kawato Y, Aonuma M, Hirota Y, Kuga H, Sato K. Cancer Res. 1991; 51:4187. [PubMed: 1651156]
37. Mohammadi R, Wassink J, Amirfazli A. Langmuir. 2004; 20:9657. [PubMed: 15491199]
38. Hesley Gina K, Gorny Krzysztof R, Henrichsen Tara L, Woodrum David A, Brown Douglas L. Ultrasound Quarterly. 2008; 24:131. [PubMed: 18528271]
39. Illing RO, Kennedy JE, Wu F, ter Haar GR, Protheroe AS, Friend PJ, Gleeson FV, Cranston DW, Phillips RR, Middleton MR. British J. Cancer. 2005; 93:890.
40. Hynynen K. J. Magn. Reson. Im. 2011; 34:482.
41. Huisman M, van den Bosch M. Cancer Imaging. 2011; 11:S166.
42. Yohe ST, Herrera VLM, Colson YL, Grinstaff MW. J. Control. Release. 2012; 162:192.

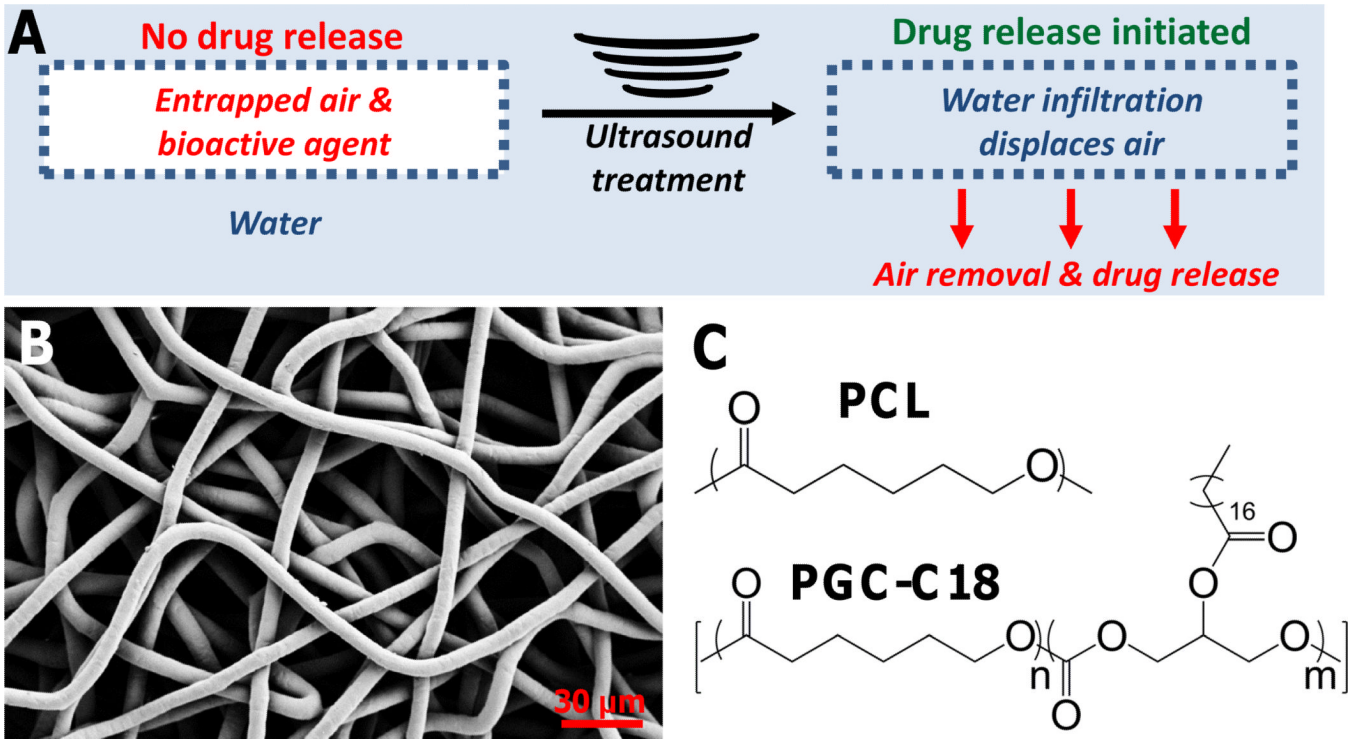

Figure 1.

(A) Proposed mechanism of drug release. Air is stable within the superhydrophobic mesh until an ultrasound treatment is used to remove the stable air layer and initiate drug release. (B) Sample PCL electrospun mesh, with average fiber sizes of 7.7 µm ± 1.2 diameter. (C) PCL and PGC-C18 were the polymers used to fabricate 3D superhydrophobic meshes.

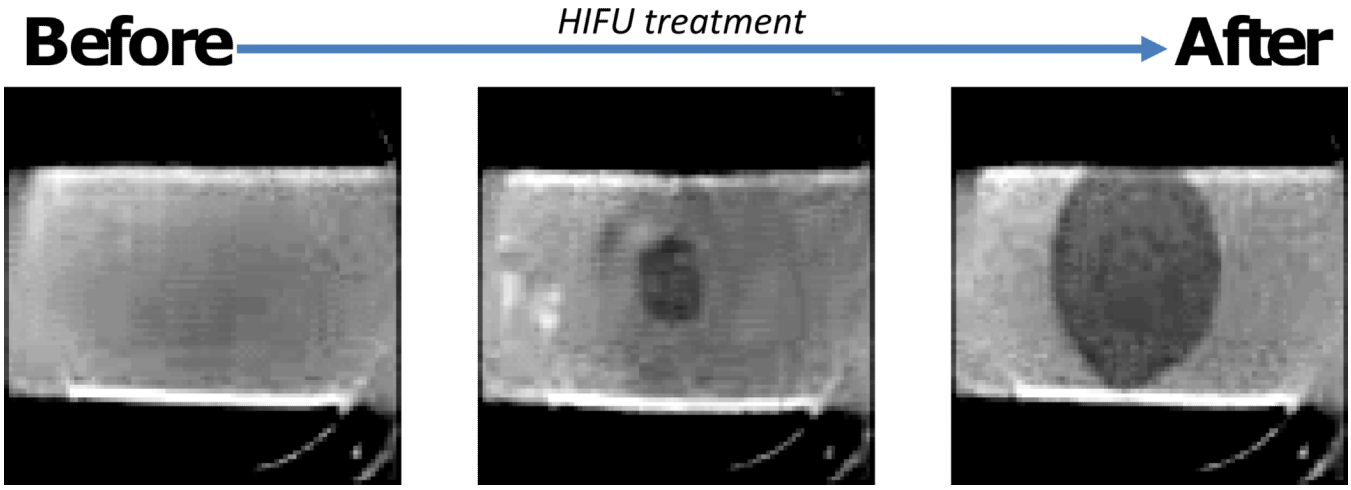

Figure 2.
Photographs of native superhydrophobic PCL electrospun meshes, where with an appropriate HIFU treatment air is removed. Meshes are opaque with air entrapped, and become transparent with water infiltration. Increased superhydrophobicity decreases the total wetted area. Photographs are in grey scale to improve contrast.

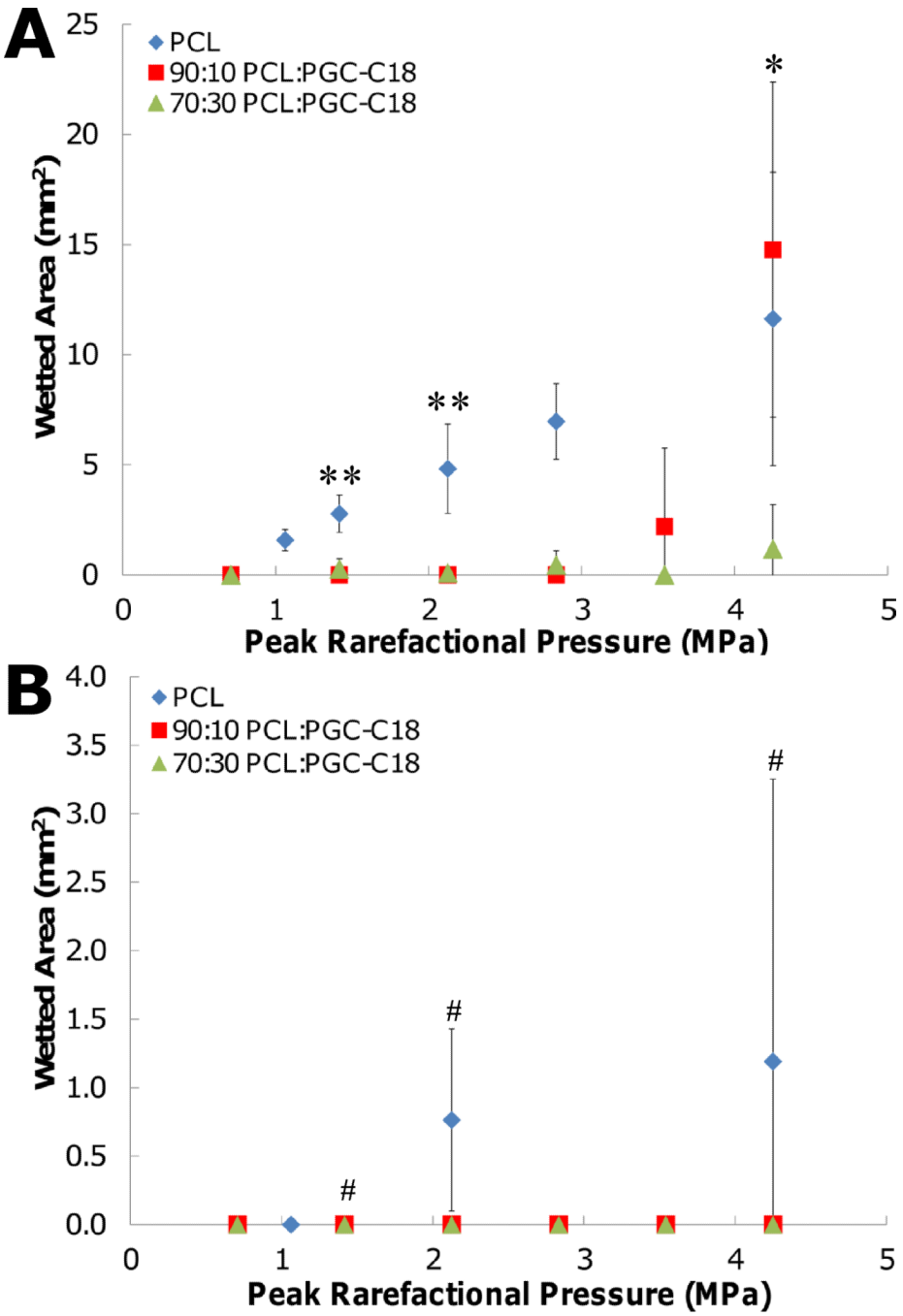

Figure 3.

Wetted area of superhydrophobic meshes as a function of peak rarefaction pressure using (A) continuous wave mode and (B) pulse mode ultrasound. Statistical significance was tested on three rarefaction pressures. (**, p-value<0.01, PCL → 10%, and PCL → 30%; *, p-value<0.05, 30% → PCL, and 30% → 10%; #, no significance) (n=3; average ± SD)

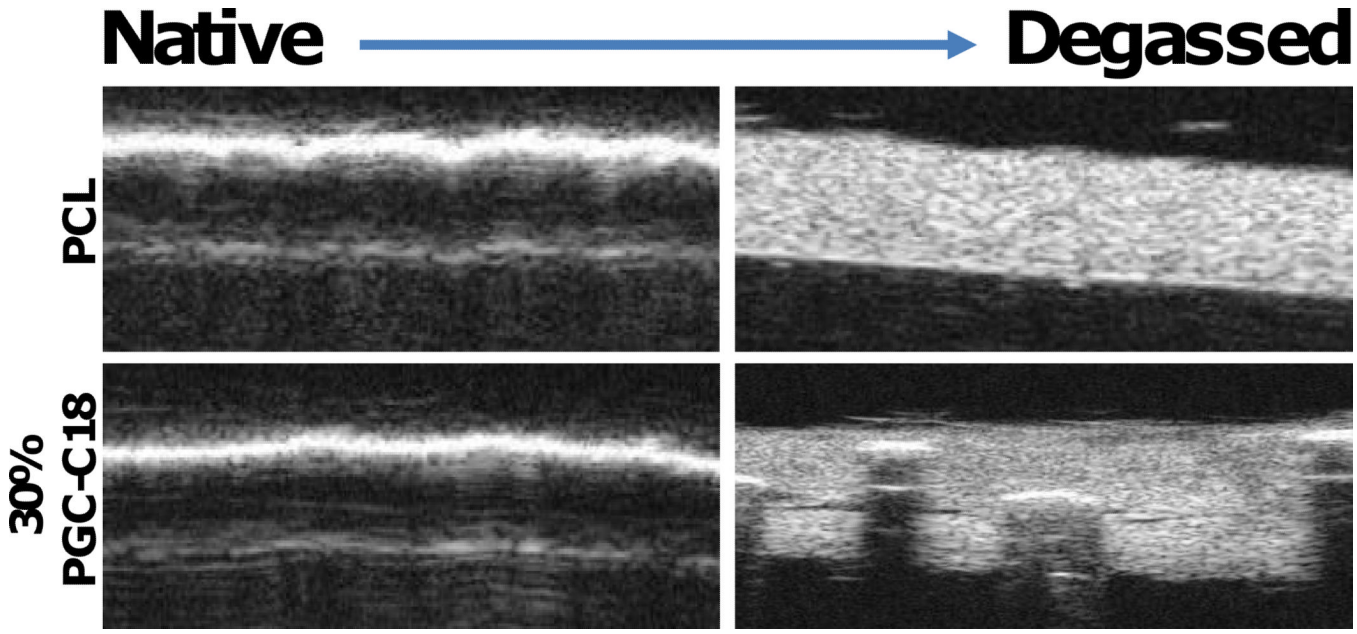

Figure 4.

Cross section of films in B-mode, showing presence of an air layer within the native materials (left), and removal of the air layer with ultrasound treatment (right). When the air layer is present, the B-mode ultrasound pulses are completely reflected off the surface and the meshes are not visible in the images. When the air layer is removed (right), B-mode ultrasound pulses pass through the surface and the meshes become visible in the images.

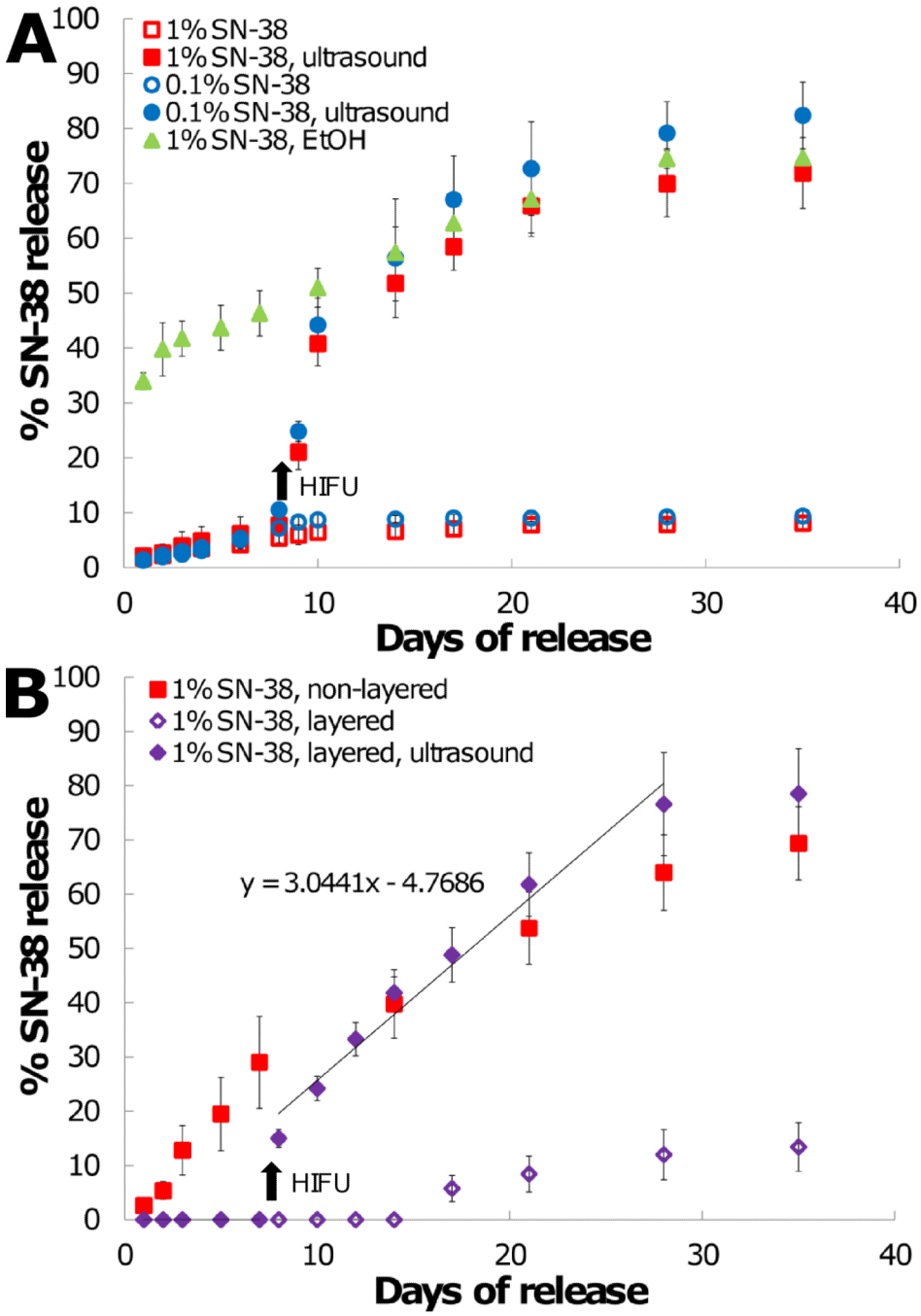

Figure 5.

(A) SN-38 release in PBS (pH 7.4) from PCL with 30% PGC-C18 meshes. An ethanol dip treatment of meshes leads to expeditious release with removal of the air layer. Native, non-degassed meshes release minimal drug, where ultrasound treatment at day 7 removes the entrapped air layer to initiate release. (B) SN-38 release from PCL with 30% PGC-C18 meshes in PBS supplemented with 10% serum. SN-38 release occurs more quickly in serum than in PBS due to a decrease in surface tension and surfactant binding. Sandwiching the drug-loaded mesh with protective non-drug loaded layers prevents SN-38 release until initiated by ultrasound treatment at day 7. Drug release eventually occurs with layered samples that were not treated with ultrasound, but in a delayed fashion. Arrows indicate time

of ultrasound treatment in both plots. Differences in SN-38 release rates from layered meshes before and after ultrasound treatment were statistically significant using analysis of covariance (ANCOVA) ($p=0.0012$). (n=3; average ± SD)

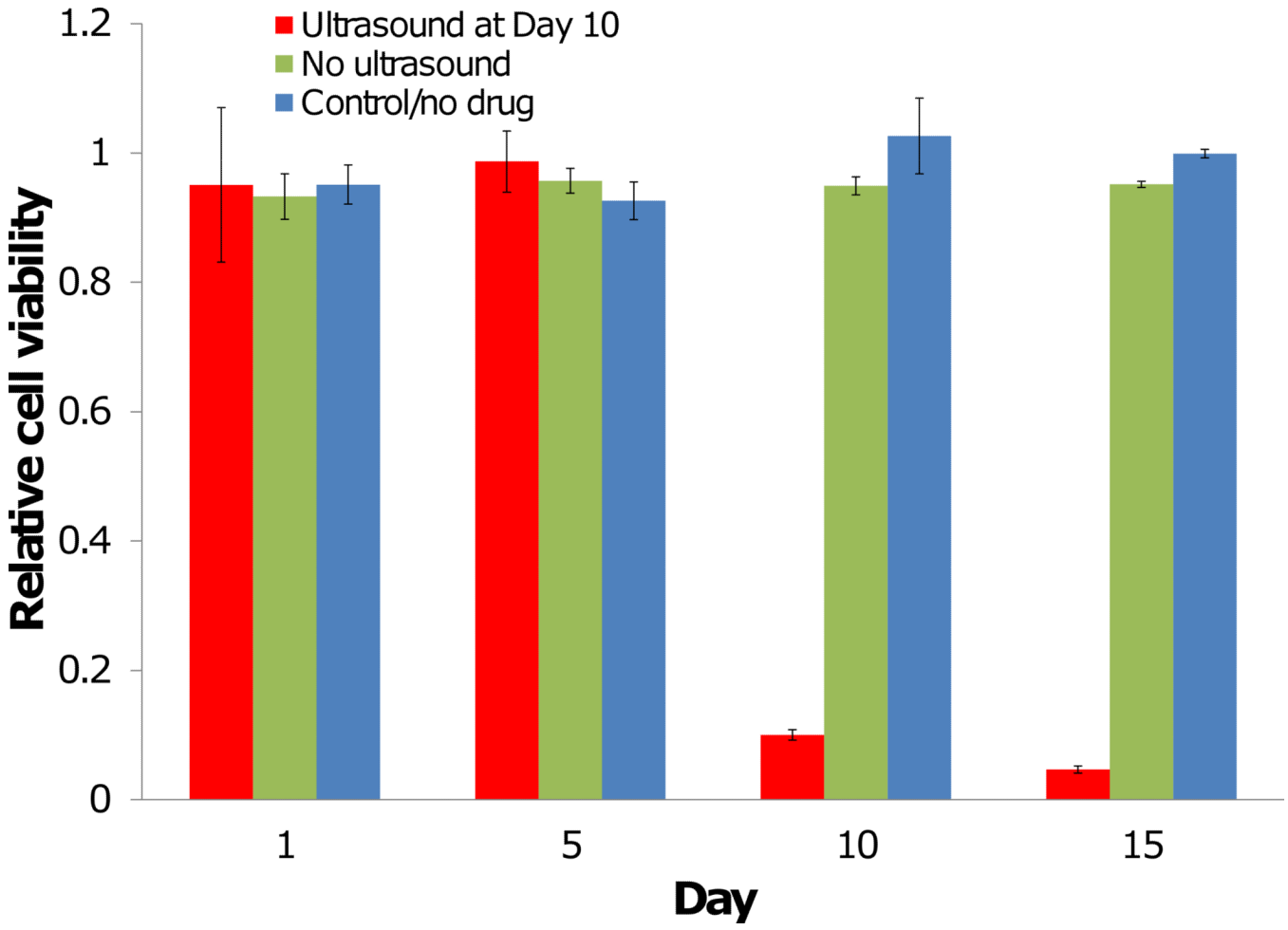

Figure 6.

Drug-loaded superhydrophobic meshes without ultrasound treatment are not cytotoxic to cells. After ultrasound treatment at day 10, SN-38 release is initiated and cancer cells are killed. Non-drug loaded meshes are not cytotoxic to cells. (n=3; average ± SD) (* = $p<0.0001$)